CHEMICAL ENGINEERING TRANSACTIONS
VOL. 106, 2023
A publication of AIDIC
The Italian Association of Chemical Engineering
Online at www.cetjournal.it
Guest Editors: Jeng Shiun Lim, Nor Alafiza Yunus, Peck Loo Kiew, Hon Huin Chin

ISBN 979-12-81206-05-2; **ISSN** 2283-9216
DOI: 10.3303/CET23106180

Towards an Understanding of the Intermolecular Interactions and Crystallographic Model of Theophylline and D-Mannitol using Synthonic Engineering Approach

Siti Nur'Aqilah Irwan[a,*], Nurul 'Atiqah Hasrin[a], Siti Fatimah Ibrahim[b], Norzahir Sapawe[a]

[a]UniKL Malaysian Institute of Chemical and Bioeng. Techn.Lot 1988 Industrial Vendor City, 78000 Alor Gajah, Malaysia
[b]School of Chemical and Process Engineering, University of Leeds LS2 9JT, Leeds, United Kingdom
snuraqilah.irwan@s.unikl.edu.my

The use of syntonic engineering (SE), or synthonic modelling has been increasing in the pharmaceutical industry. This study used the Material Studio and HABIT98 programs to model the intermolecular (synthonic) interactions, lattice energetics, and morphology prediction. Two organic systems representing common active ingredients and excipients were selected, Theophylline (TH) and D-mannitol (DM). The Nemethy and Dreiding force fields (FF) paired with matching semiempirical chargers were used for all SE calculations for all case studies. For both systems, hydrogen bonding OH…H was the dominating interaction. The interatomic stability for TH was mainly contributed by the amino nitrogen making amide the primary functional group. In DM, interatomic stability was attributed to the hydrogen atom, making hydroxyl the primary functional group. TH was crystallised as needle-like, while DM was dendritic.

1. Introduction

The substantial interest in rationally designing crystal's bulk properties through manipulating molecular substituents and supramolecular solid-state structure is the foundation of crystal engineering. Crystal engineering is a promising method for describing molecular crystals, particularly pharmaceutical particulates (e.g., active pharmaceutical ingredient (API) and excipient) and improving their physicochemical properties. Thereby, detailing the molecular synthonic interactions can lead to a better elucidation of the material's properties, which paves the route for better processing quality.

Consequently, the SE method has been utilised to a great extent to foresee crystal morphologies and the bulk (intrinsic) and surface (extrinsic) synthons interactions using empirical FF methods (Nguyen et al., 2020). This approach is consistently applied to crystals by considering a central molecule and summing the molecular interaction energy of a pair of atoms between two interacting molecules within a given convergence radius (Pickering et al., 2017). Molecular interactions such as Van der Waals (VdW) and electrostatic potential are of utmost importance to describe intermolecular synthons between two species. The charge distribution of an isolated molecule is valid for describing the charge distribution of a bulk crystal molecule (Anuar et al., 2022).

This study reports the computational analysis of solid form synthons and their predicted morphologies. TH and DM are presented to demonstrate the importance of understanding crystallographic structures that are potentially governing the solid-state architecture for designing pharmaceutical drug formulation and crystal engineering.

2. Materials and methods

2.1 Preparation of crystal structures

The molecular structures of (i) TH, $C_7H_8N_4O_2$; CCDD (Cambridge Crystallographic Data Centre) reference code 7232823 (Larsen et al., 2019), and (ii) DM, $C_6H_{14}O_6$; CCDD reference code 224660 (Fronczek et al.,

Paper Received: 05 March 2023; Revised: 25 July 2023; Accepted: 11 October 2023
Please cite this article as: Irwan S.N., Hasrin N.`., Ibrahim S.F., Sapawe N., 2023, Towards an Understanding of the Intermolecular Interactions and Crystallographic Model of Theophylline and D-Mannitol using Synthonic Engineering Approach, Chemical Engineering Transactions, 106, 1075-1080 DOI:10.3303/CET23106180

2003), were retrieved from Cambridge Structural Database. TH has a primitive monoclinic crystal structure with a space group of *P 1 2₁/c 1* in the unit cell. The cell dimensions were, *a* = 4.531, *b* = 11.578, *c* = 15.719 and *β* = 93.69 °. On the other hand, the DM molecule was packed in an orthorhombic lattice with space group P 2_1 2_1 2_1 in unit cell dimensions; *a* = 4.899, *b* = 18.268, *c* = 5.043 Å and *β* = 118.39 °. TH and DM structures were optimised with respect to the potential energy i.e., *COMPASS-II and Drieding (Mayo et al., 1900), respectively, using* ACCERLYS Materials Studio software to a stable geometric configuration (BIOVIA, 2017).

2.2 The selection of potential (Force Field) set

In this work, *the combination of Nemethy* FF (Némethy et al., 1983) with MOPAC-PM3 was applied to TH. For DM, the *Drieding II* FF (Mayo et al., 1990) and Gasteiger charges were used for all calculations.

2.3 Crystal chemistry analysis

2.3.1 Lattice energy, interatomic and intermolecular Interactions

Crystal lattice energy (E_{latt}) was calculated with limiting radii ranging from 20 to 100 Å using the HABIT98 program (Clydesdale et al., 1996). The calculated E_{latt} and sublimation enthalpy (ΔH_{sub}) are related through Eq(1) (Ouvrardt & Mitchell, 2003).

$$E_{latt} = \Delta H_{sub} + 2RT \quad (1)$$

2RT denotes a correction factor for the difference between the gas enthalpy and the vibrational contribution to the crystal enthalpy. The calculated E_{latt} is also used to assess the reliability of the selected FF concerning the solid forms.

2.3.2 Crystal morphology prediction

The prediction of crystal morphologies and growth faces of molecular systems were calculated by three different morphological methods of the Material Studio program (BIOVIA, 2017), i.e. (i) Bravais Friedel Donnay Harker (BFDH) rules, (ii) growth morphology (GM), and (iii) equilibrium morphology (EM), with the suitable FFs and the charges at medium quality setting.

2.4 Slow evaporation crystallisation

The slow evaporation method was used with a solubility of TH; 30 mg/ml (Bobrovs et al., 2015) and DM;400 mg/ml (Poornachary et al., 2013) in a water solvent. The solution was naturally cooled to the ambient temperature, by allowing water vapour to escape through holes punched in aluminium foil placed on the top of the beakers. The solution was harvested for crystals and then filtered to remove the crystals.

3. Results and discussions

3.1 Crystal lattice energies calculations

The E_{latt} (using HABIT98) for TH and DM converged at 96.48kJ/mol and 126.06kJ/mol, as in Figure 1. Both calculated E_{latt} were in good agreement with the former experimental sublimation enthalpy i.e., 126 kJ/mol for TH (Fokkens et al., 1983) and 202 kJ/mol for DM (Barone et al., 1990) with 5.26 % and 2.40 % difference.

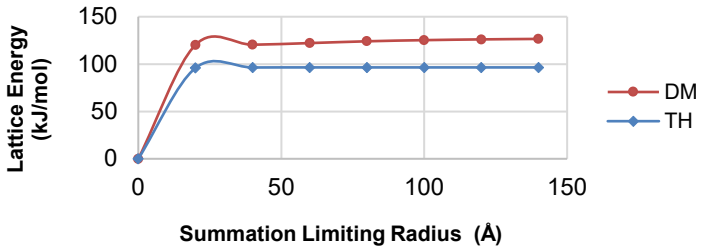

Figure 1: Lattice energy convergence analysis using HABIT98 program for TH and DM crystal structures

3.2 Interatomic interaction and functional contribution

TH interatomic stability is driven by amino nitrogen with a significant contribution; of -29.25 kJ/mol to $E_{latt.}$ Besides amino nitrogen, the two most important contributions were carbonyl carbon and carbonyl oxygen type of atom with a total energy of -17.03 kJ/mol and -15.73 kJ/mol. These carbonyl groups are known as polar groups. The main functional group contribution to the TH is the Amide with 44.8 % reflecting its close association with forceful coulombic interaction between anions and cations. Followed by aliphatic (22.97 %), methyl (18.61 %), imine (8.53 %) and alkene (5.05 %) (Refer to Figure 2). The stability of amide bonds is due to their tendency to form

a resonating structure towards various reaction conditions, high temperatures, and the presence of other chemicals. Literature indicates that compounds with amide pharmacophore have a more comprehensive range of pharmacological actives, including anti-inflammatory, which is in line with the function of TH as a systemic anti-inflammatory agent (Barnes, 2010).

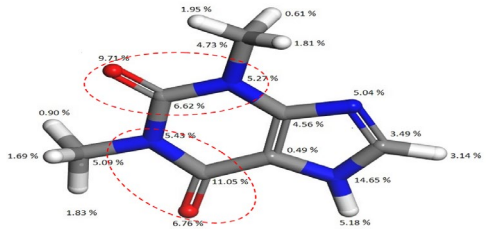

Figure 2: Functional group of TH. The dotted line denotes the major functional group i.e, Amide

On the other hand, the specific percent for atom's contributions towards the stability of the DM molecular structure was dominated by hydrogen type of atom. Hydrogen atom with involved hydrogen bonding (H-bond) contributes the significant contribution in DM molecular crystal with -206 kJ/mol of total energy. While the most minor atom's contribution is goes to carbon atom (-28.41 kJ/mol). Figure 3 depicts the percentage distributions of individual atoms in the DM molecule. The summation of the atom and associates functional group revealed that the hydroxyl group (-OH) contributed the most to the calculated E_{latt}, i.e., 80.71 %, followed by the aliphatic group with 19.29 % of distributions. Like amides, -OH groups can form hydrogen bonds. Hence, the contribution of abundant OH groups in DM structure makes it an ideal excipient with highly hydrating properties, enhancing water solubility when interacting with active compounds. Due to that, the suitability of DM for emerging formulation technology of orally disintegrating tablets has been recently pointed out.

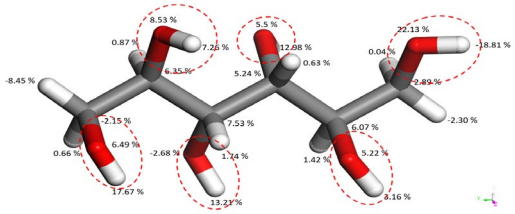

Figure 3: Functional group of DM. The dotted line denotes the major functional group i.e., Hydroxyl (-OH)

3.3 Intermolecular synthon analysis

Tables 1 and 2 summarise TH and DM intermolecular synthon breakdown into attractive, repulsive, coulombic intermolecular energy. Results show that each molecule's top attractive synthons were created to be between the anion-cation pairs, reflecting the dominant interactions resulting from the coulombic forces. In the TH molecule, the strongest interaction was the H-bong (H…O) network depicted in synthon A between the aliphatic hydrogen donor (-H) group and carbonyl oxygen (C=O), as shown in Figure 4. The strength of the interaction was -16.86 kJ/mol in [-1 0 0], with 4.53 Å. Although synthon B of bond formation has a similar distance as synthon A, its total energy has slightly differed. Besides the H-bond, the TH molecule was governed by the VdW forces. The VdW bond formation exists between two molecules of hydrogen and carbon atoms (as in synthon C), H-H bond (H...H) (synthon E and F), and nitrogen-nitrogen bond (N...N) present in synthon G. The directionality of the H-bond (depicted in synthon A, B and D) explains the elongation of the crystal forming the columnar habit. While weaker interactions like VdW forces are readily broken and displaced.

Table 1: Details of the top seven intermolecular synthons in the crystal structures of theophylline.

Synthons	Multiplicity	Distance (Å)	Attractive (kJ/mol)	Repulsive (kJ/mol)	Coulombic (kJ/mol)	Total Intermolecular Energy (kJ/mol)	Intermolecular Interaction Type
A	4	4.53	-25.02	8.83	-0.67	-16.86	H-Bond
B	4	4.53	-24.98	8.87	-0.67	-16.77	H-Bond
C	4	7.24	-11.72	4.60	-3.47	-10.59	VdW
D	4	5.37	-20.21	8.74	1.13	-10.33	H-Bond
E	4	7.27	-10.96	6.15	0.13	-4.69	VdW
F	4	8.88	-5.02	3.56	-2.97	-4.44	VdW
G	4	8.88	-4.90	3.56	-2.97	-4.31	VdW

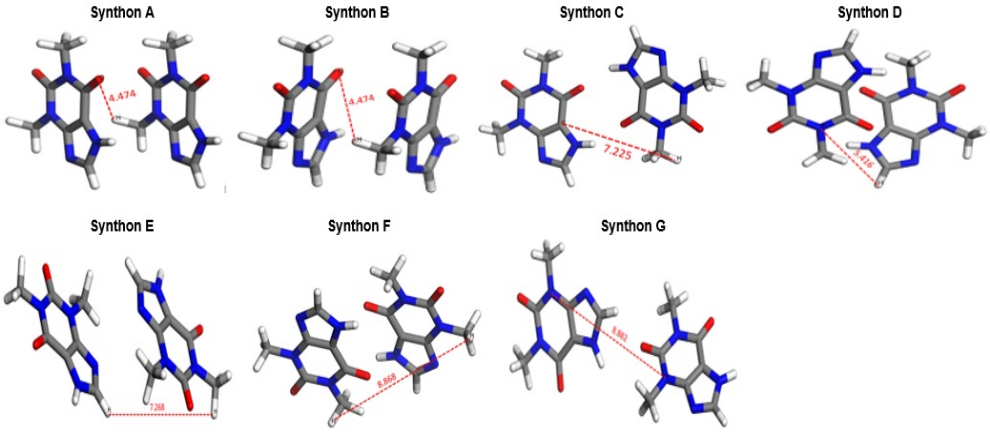

Due to the DM molecular structure terminal nature exposing -OH group, most of the intermolecular synthon energies created were H-bonds. As shown in Figure 5, the strongest interaction of H-bond was created by synthon A with the shortest distance, i.e., 4.85 Å (shown is the closest value to the calculated distance, 4.90 Å), and followed by synthon C, distance elongated to 5.04 Å and synthon B with the closest distance value obtained, 5.07 Å to the calculated value (5.09 Å). The total intermolecular energy is dominated by attractive forces in the molecules. Hence, due to the high polarity created in a DM crystal, it is often assumed to be the hardest to displace.

Table 5: Details of the top three pairwise intermolecular synthons in the crystal structures of D-mannitol

Synthons	Multiplicity	Distance (Å)	Attractive (kJ/mol)	Repulsive (kJ/mol)	Coulombic (kJ/mol)	Total Intermolecular Energy (kJ/mol)	Intermolecular Interaction Type
A	4	4.90	-158.3	144.83	-7.61	-21.00	H-Bond
B	4	5.09	-49.08	39.20	-6.36	-16.19	H-Bond
C	4	5.04	-13.63	45.44	-1.30	-12.89	H-Bond

Figure 5: The dominant pairwise intermolecular bonding of D-mannitol molecule showing their respective distance (Å) between two atoms by lines.

3.4 Morphologies prediction analysis

The comparative analysis of TH morphology shows that BFDH and GM tools simulate TH crystal with the same number of crystal habits, i.e., six facets. While EM visualises the crystal habit up to thirty-six facets. In Figure 6, TH crystals show a needle-like morphology dominated by the {011} face. The {011} face shows a layer of the -OH group exposed on their surfaces, making them relatively favourable to hydrophilic and potential interactions (shown in Figure 7). TH predicted morphology was like observed grown crystals.In DM (Figure 8), the GM method depicts the simplest prediction of DM crystal structure with the fewest crystal habits, i.e., seven facets. The structural complexity increases with the following method of BFDH, with eleven crystal facets, and EM, with thirty crystal facets. DM morphology is generally dominated by the (020) face having the largest facet areas.

The cleaved (020) face exposed the numbers of -OH groups (Figure 9). The morphology produced by these three methods has hexagonal plate-like morphology, which contrasts with dendritic-grown crystals. The experimental crystals show the closest structure to the BFDH method among the three prediction crystals. However, the measurement technique used could be more efficient.

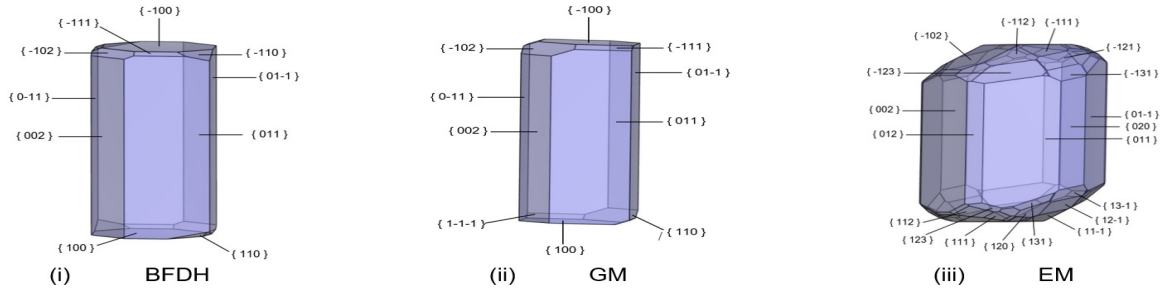

Figure 6: The comparative morphological analysis for theophylline crystal compound.

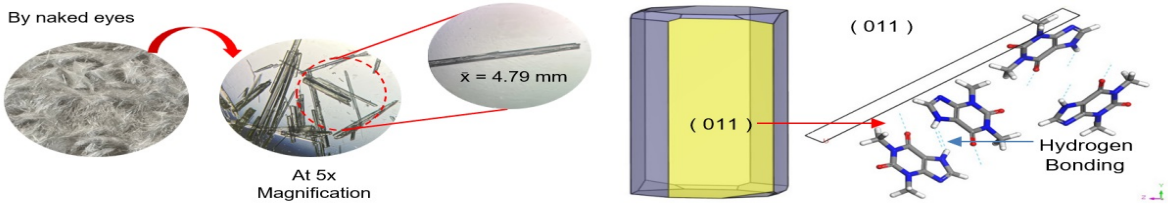

Figure 7: The correlation of predicted TH crystal and experimental observation 5x magnification. Followed by the relationship of TH crystal morphology and its dominant surface chemistry, { 011 }.

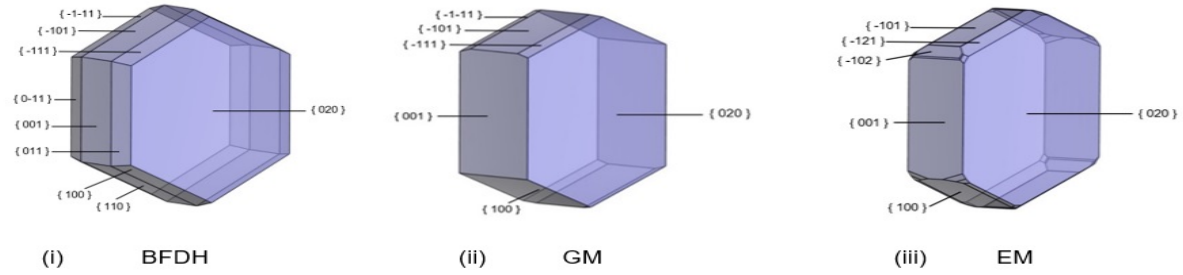

Figure 8: The comparative morphological analysis for D-mannitol crystal compound.

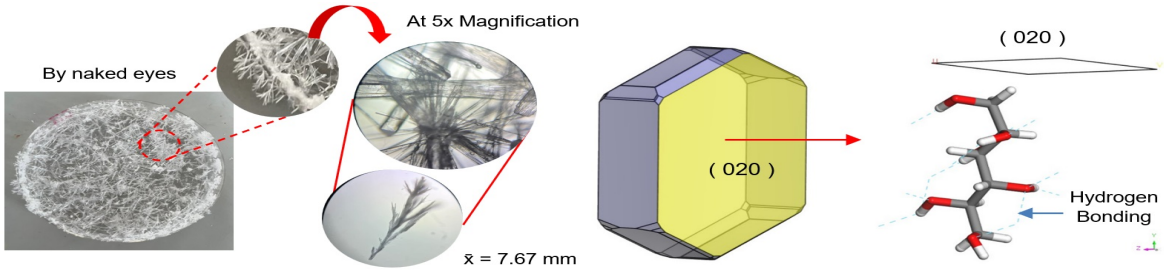

Figure 9: The correlation of predicted DM crystal and experimental observation 5x magnification. Followed by the relationship of DM crystal morphology and its dominant surface chemistry, { 020 }.

4. Conclusions

The results of E_{latt} and their contributions to TH and DM crystals from intermolecular synthonic and crystallographic perspectives have been elucidated here. Using a SE approach, each system's E_{latt} and morphology prediction has been successfully carried out with the appropriate FFs and atomic charges method.

It was observed that TH created dimer hydrogen bonds between O…H atom and multiple undirected nature of VdW interactions, which can give rise to a polymorphism. On the other hand, DM molecular structure terminal nature exposes the -OH group. Hence, most intermolecular synthon energies created were H-bonding. The predicted morphology then was compared with the experimental shape in which TH crystal showed good agreement; nonetheless, it is vice versa to DM crystal in which recommended using SEM. Overall, a mechanistic understanding of pharmaceutical material's behaviour is essential for controlling their physicochemical properties. This, in turn has the potential to improve the process of developing new drugs underpinning the crystal chemistry and crystallographic study of solid dosage formulations in future work.

Acknowledgment

This work was kindly one part of the project that was generously supported by the Fundamental Research Grant Scheme (FRGS), reference code FRGS/1/2021/TK0/UNIKL/02/7.

References

Anuar N., Yusop S. N., Roberts K. J., 2022, Crystallisation of organic materials from the solution phase: A molecular, synthonic and crystallographic perspective, Crystallography Reviews, 28, 97-215.

Barnes P. J., 2010, Theophylline, Pharmaceuticals, 3(3), 725–747.

BIOVIA, 2017, Materials Studio, Revision 8.0, Accelrys Inc., San Diego: Dassault Systemes.

Bobrovs R., Seton L., Dempster N., 2015, The reluctant polymorph: Investigation into the effect of self-association on the solvent mediated phase transformation and nucleation of theophylline, CrystEngComm, 17(28), 5237–5251.

Clydesdale G., Roberts K. J., Docherty R., 1996, HABIT95 - A program for predicting the morphology of molecular crystals as a function of the growth environment, Journal of Crystal Growth, 166(1–4), 78–83.

Coombes D. S., Richard A., Catlow C., Gale J. D., Hardy M. J., Saunders M. R., 2002, Theoretical and experimental investigations on the morphology of pharmaceutical crystals, Journal of Pharmaceutical Sciences, 91(7), 1652–1658.

Fokkens J. G., van Amelsfoort J. G. M., de Blaey C. J., de Kruif C. G., Wilting J., 1983, A thermodynamic study of the solubility of theophylline and its hydrate, International Journal of Pharmaceutics, 14(1), 79–93.

Fronczek F. R., Kamel H. N., Slattery M., 2003, Three polymorphs (α, β, and δ) of d-mannitol at 100 K, Acta Crystallographica Section C: Crystal Structure Communications, 59(10), 567–570.

Mayo S. L., Olafson B. D., Goddard W. A., 1990, DREIDING: A generic force field for molecular simulations, Journal of Physical Chemistry, 94(26), 8897–8909.

Némethy G., Pottle M. S., Scheraga, H. A., 1983, Energy parameters in polypeptides. 9. Updating of geometrical parameters, nonbonded interactions, and hydrogen bond interactions for the naturally occurring amino acids, Journal of Physical Chemistry, 87(11), 1883–1887.

Nguyen T. T. H., Hammond R. B., Styliari I. D., Murnane D., Roberts K. J., 2020, A digital workflow from crystallographic structure to single crystal particle attributes for predicting the formulation properties of terbutaline sulfate, CrystEngComm, 22(19), 3347–3360.

Larsen A. S., Olsen M. A., Moustafa H., Larsen F. H., Sauer S. P. A., Rantanen J., Madsen A., 2019, Determining short-lived solid forms during phase transformations using molecular dynamics, CrystEngComm, 21(27), 4020–4024.

Othman M. F., Anuar N., Yusop S. N. A., Md Azmi N. S., Nurul N. A., 2019, Morphology prediction and dissolution behaviour of α-succinic acid in ethanol solution using molecular dynamic simulation, Key Engineering Materials, 797, 139–148.

Ouvrardt C., Mitchell J. B. O., 2003, Can we predict lattice energy from molecular structure?, Acta Crystallographica Section B: Structural Science, 59(5), 676–685.

Pickering J., Hammond R. B., Ramachandran V., Soufian M., Roberts K. J., 2017, Synthonic engineering modelling tools for product and process design, NATO Science for Peace and Security Series A: Chemistry and Biology, PartF1, 155–176.

Poornachary S. K. P., Parambil J. V., Chow P. S., Tan R. B. H., Heng J. Y. Y., 2013, Nucleation of elusive crystal polymorphs at the solution-substrate contact line, Crystal Growth and Design, 13(3), 1180–1186.